

The evolution of Information entropy components in Relativistic Heavy-Ion Collisions

Fei Li¹ and Gang Chen^{1,*}

¹*School of mathematics and physics, China University of Geosciences(Wuhan), Wuhan 430074, China*

Shannon information entropy provides an effective tool to study the evolution process in relativistic heavy-ion collisions. The time evolution process of thermodynamic entropy S_{thermal} , multiple entropy S_{mul} , and configuration entropy S_{conf} at RHIC is studied using the AMPT model to generate central Au-Au collisions. By superimposing the three kinds of information entropy, we can get a more complete information entropy of the system to describe the physical information of the relativistic heavy ion collision. The results show that the four stages of the time evolution process of the system entropy S seem to correspond to the four physical processes in the relativistic heavy ion collision, indicating that the total entropy of the system can reflect the physical information in the relativistic heavy ion collision more accurately.

PACS numbers: 25.75.Nq, 24.10.Lx, 24.60.Lz, 89.70.+c

I. INTRODUCTION

Search for clear signatures of the phase transition in Relativistic heavy-ion collisions (RHIC) is an important subject in high-energy physics. The process of phase transition in collisions at RHIC includes the transformation of quark-gluon plasma (QGP) into hadron gas. Physicists believe that this process reproduces the situation of the first 10s after the Big Bang [1]. Further study of phase transition can bring a deeper understanding of the properties of the nuclear matter produced in the interaction of heavy nuclei and the mechanism of the origin of the universe. However, due to the complexity of the dynamic properties of the phase transition process in heavy-ion collisions, there is no unified theory to describe the whole reaction process at present. In this dilemma, researchers use different theoretical approaches to describe different stages in nuclear collisions [2], and some researchers simultaneously devoted themselves to the study of entropy generated in collision process by using different dynamic models in the 1980s [3]. In recent studies, Shannon information entropy has been adopted and developed by some researchers because it provides a new method and observation [4].

Based on the works [5–8] of Boltzmann and Gibbs in the last 20 years of the 19th century, today we understand that the entropy of the system can be determined by its specific probability distribution p_i , for a system in state i . In 1948, C.E. Shannon discovered a theorem similar to the definition of “entropy” in physics, which can be expressed as follows [9, 10]:

$$S = -k_B \sum_i p_i \ln p_i \quad (1)$$

where p_i ($i=1, 2, \dots, n$) is the independent probabilities of events in a system and k_B is Boltzmanns constant. For a given set of constraints, when p_i is the most probable

state of the system, the information entropy has a maximum value. In terminology of physics, when the system is in the most probable distribution, its entropy is the maximum, which corresponds to its equilibrium state. It should be noted that the above definition of entropy is very broad, which can be used not only for the equilibrium state of the system, but also for the non-equilibrium state of the system.

The Shannon information entropy has been applied and developed in many scientific areas [4]. In the area of heavy-ion collisions, Cao and Hwa first applied Shannon information entropy to the study of chaotic behavior caused by particle production in branching process [11]. In 1996, Y.G. Ma adopted the idea of “event entropy” to obtain a novel signature of liquid gas phase transition under the references of transition temperature in 1999 [12]. In the study of intermediate mass fragments, C.W. Ma et al. adopted the event information entropy found the isobaric scaling phenomenon in neutron-rich projectile fragmentation reactions [13], as well as, in the fragments differing of different neutron-excesses [14]. Recently, J. Xu and C.M. Ko investigated the chemical freeze-out conditions in RHIC by specific entropy of hadrons [15].

In the process at RHIC, the scattering between particles, the production and annihilation of particles, and the variation of the internal structure of particles are always accompanied. Because information entropy can be expressed by different stochastic variables in different physical conditions, it is suitable to adopt the thermodynamic entropy, multiplicity entropy, and configuration entropy to describe these different types of information changes. Here, the distribution $\{p_i\}$ of thermodynamic entropy is defined by the distribution of 6-dimensional phase space of particles, which measures the disorder degree of particles in phase space, and the distribution $\{p_i\}$ of multiplicity entropy is defined by the event probability of having i particles produced, which measures the disorder of particles in event phase. The adoption of configuration entropy in this work is inspired by Csernai et al. [16] and Lichtenberg [17], makes us consider the information variables generated by the different composition of quarks inside hadrons, because hadrons are not

*Electronic address: chengang1@cug.edu.cn

a point particle. The introduction of these three different entropies will be detailed in the following section.

The organization of the present letter is as follows. In section 2, The A multiphase transport model (AMPT), which we used in this work, will be briefly introduced. In section 3 and 4, the thermodynamic entropy and multiplicity entropy in the evolution of heavy-ion collisions is investigated. In section 5, the configuration entropy of hadron internal structure will be introduced, the configuration entropy and the total information entropy in the evolution of heavy-ion collisions is investigated as well.

II. THE AMPT MODEL

A multiphase transport model [18] is used to analyze the evolution of information entropy, which is a widely used theoretical tool for relativistic heavy ion collisions. The AMPT model is based on nonequilibrium transport dynamics, which consists of four parts: the Heavy-Ion Jet Interaction Generator (HIJING) model [19] for generating the initial-state information, Zhangs parton cascade (ZPC) model [20] for modeling partonic scatterings, the Lund string fragmentation model or a quark coalescence model for hadrons formation, and a relativistic transport (ART) model [21] for treating the resulting hadron scatterings. These are combined to give a coherent description of the dynamics of relativistic heavy ion collisions.

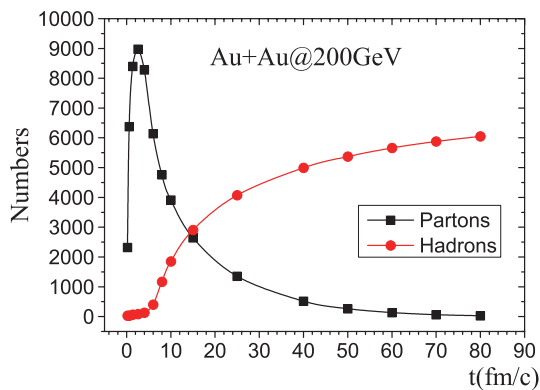


FIG. 1: Time evolution of the parton and hadron production in the central Au+Au collisions at $\sqrt{s_{NN}} = 200$ GeV calculated by AMPT.

Here we choose the string melting version of the AMPT model (v2.26t9b;isoft=5), in which partons freeze-out according to local energy density. The hadronization process is realized by a quark cascade model, which combines two nearest partons into a meson and three nearest quarks (anti-quarks) into a baryon (anti-baryon). The method of determining hadron species is done by the flavor and invariant mass of coalescing partons. The impact parameter is in the range $b \leq 3$ fm and the parton cross section is taken to be 10 mb. To give a general

picture of the evolution of particle production after collision, we obtain the time evolution of the number of partons and hadrons in the central Au+Au collision at the $\sqrt{s_{NN}} = 200$ GeV by using AMPT. As shown in Fig. 1, a large number of partons are produced in the early stage of collision ($t < 5$ fm/c), while later only a few hadrons are produced. During these times, partons are dominant, and the whole system is in a deconfined phase, which is in the perturbative QCD vacuum, with only a few of hadrons [22]. After that, the number of hadrons increases with the decrease of the number of partons, and the system goes through a phase transition into hadron gas phase.

III. THE THERMODYNAMIC ENTROPY

The thermodynamical entropy can be calculated by the 6-dimensional phase space distribution $p_i(p_x, p_y, p_z, x, y, z)$. Under the definition of shannon entropy, the p_i is the ratio of the particle number in the local 6-dimensional phase-space i.e. the i -th bin in the global 6-dimensional phase space. Here, the number and size of 6-dimensional phase space units are set to sufficiently contain all the mechanical information after the average of all events. It should be noted that the distribution of the system is based on the number of certain particles versus the total number of particles. The thermodynamic entropies of the partons, hadrons, and system are calculated by Eq. (1) in Au+Au collisions at $\sqrt{s_{NN}} = 64.2$ GeV, 200 GeV, and 800 GeV.

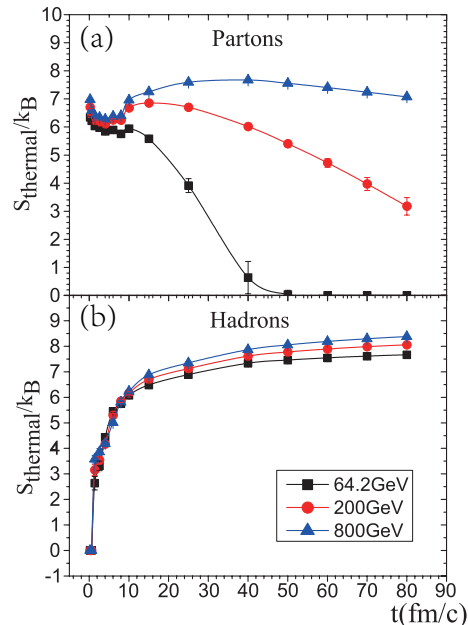


FIG. 2: Time evolution of thermodynamic entropy in Au+Au collisions at different c.m. energies for (a) partons and (b) hadrons.

We can be seen from Fig. 2(a), that the thermody-

dynamic entropy of partons at different center of mass energies (c.m. energy) have similar evolution curves. The trend of the thermodynamic entropy decreases first, then goes up and reaches a vertex, and then decreases. The reason for the decrease of parton thermodynamic entropy in the first stage is that strings are not included in our statistics, and then the energy released by the string melting is used as the external energy input to the system. The increase of the thermodynamic entropy of partons in the second stage is due to the scattering and generation of partons. The decrease of thermodynamic entropy of partons in the third stage is due to the disappearance of cooling of partons. It can be observed that the thermodynamic entropy of the final parton disappears earlier in low-energy collisions because the central local temperature is lower in low-energy collisions, so the partons freeze out faster.

From Fig. 2(b), the thermodynamic entropy of all hadrons increase rapidly in the early stage at three different c.m. energies, due to the rapid generation of hadrons. Then, the thermodynamic entropy of hadrons gradually tends to saturation and reaches a maximum, which means that the system tends to equilibrium.

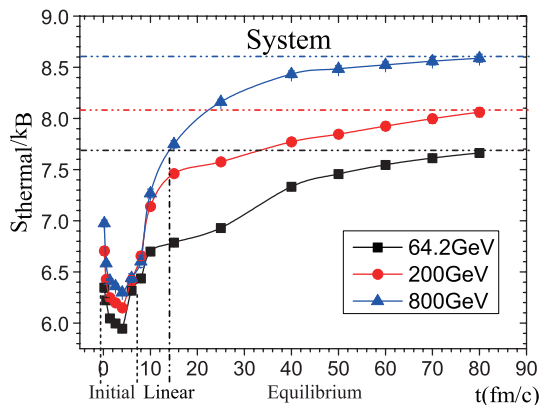


FIG. 3: Time evolution of thermodynamic entropy for system in Au+Au collisions at different c.m. energies.

Fig. 3 shows the time evolution of thermodynamic entropy for the whole collision system, which goes through three stages. The first stage is the initial state of parton, its total thermodynamic entropy decreases and increases due to the energy released and gained by string formation and melting. It also can be interpreted in physical images as entropy reduction caused by compression and expansion after collision. At the same time, the quark gluon plasma (QGP) is formed when the entropy decreases to the minimum. In the second stage, the thermodynamic entropy linearly increases at $t = 5$ to 10 fm/c, which corresponds to the phase transition process of the system from QGP to hadronic gas. The third stage is the process of thermodynamic entropy approaching saturation, which corresponds to the final equilibrium state of hadron scattering. In addition, the higher the c.m. energy in the high-energy collision, the faster the thermodynamic en-

ropy of the system reaches the equilibrium state. This is because the particles produced by collisions with higher energies have higher momentum, which makes the system approach the maximum disorder faster.

IV. THE MULTIPLICITY ENTROPY

Above we studied the time evolution of thermodynamic entropy in high-energy collision systems. In fact, there is also a multiplicity entropy in high-energy heavy ion collisions. In 1999, Y.G. Ma introduced this method [12] to diagnose a nuclear liquid gas phase transition by multiplicity entropy, which determines the critical point by finding the maximum value of multiplicity entropy in a certain state of the system. Here, in the context of multiplicity entropy, the probability distribution p_i is related to the ratio of the particle numbers N_i produced in the i -th bin to the total particle number N , i.e. $p_i = N_i/N$. p_i is the normalized probability distribution, where $\sum_i p_i = 1$. The time evolution of the multiplicity entropy of partons and hadrons at different c.m. energies is calculated by Eq. (1), as shown in Fig. 4.

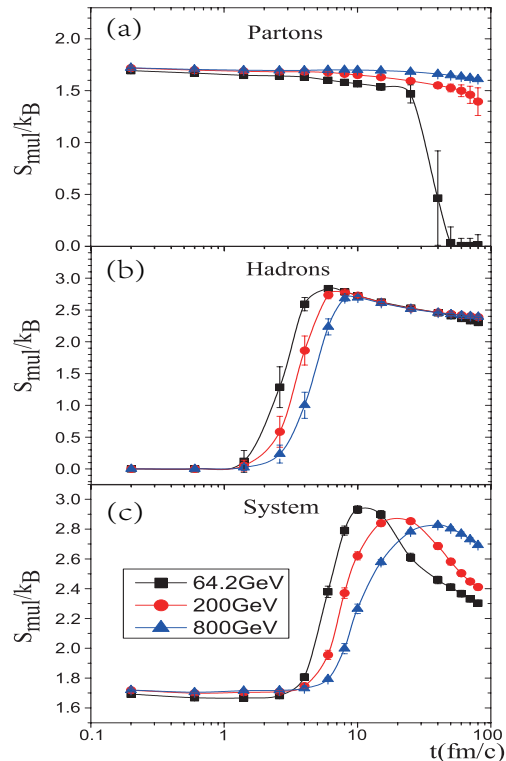


FIG. 4: Time evolution of multiplicity entropy in Au+Au collisions at different c.m. energies for (a) partons, (b) hadrons, and (c) system.

From Fig. 4(a), we can see that the time distribution of multiplicity entropy of partons are all similar under different c.m. energies of Au-Au collisions. The multiplicity entropy of partons decreases slowly before 10 fm/c

of the evolution process, which is due to the fact that the distribution of various kinds of partons remains almost unchanged at this stage. Under the conditions of $\sqrt{s_{NN}} = 200$ GeV and 800 GeV, the multiplicity entropy of partons decreases slightly after 10 fm/c, which is due to the faster cooling of energetic quarks at the later stage of the collision system. Under the condition of $\sqrt{s_{NN}} = 800$ GeV, the change of multiplicity entropy is smaller than that of $\sqrt{s_{NN}} = 200$ GeV, because the energetic quarks can exist longer under higher energy collisions, which has little effect on the overall distribution of partons. At $\sqrt{s_{NN}} = 64.2$ GeV collisions, the multiplicity entropy drops sharply near 30 fm/c because the partons almost completely freeze out.

In Fig. 4(b), a significant inflection point appears about 6-8 fm/c of hadronic multiplicity entropy, which is the maximum of multiplicity entropy at different c.m. energies. This seems to imply the critical point of the system from QGP to hadronic gas. This inflection point gives a good sign of phase transition because the maximum of the multiplicity entropy reflects the largest fluctuation of the multiplicity probability distribution at the critical point. From the perspective of information theory, the prediction of which hadron will appear in the system at this moment is the most difficult. Fig. 5(a) shows that the maximum value of multiplicity entropy appears at about 7 fm/c, and the corresponding temperature in Fig 5(b) at the same time is 147 MeV, which is almost the same as the chemical freeze-out temperature of 141 MeV obtained by specific entropy in reference [15]. Both results are slightly lower than those extracted from the experimental data based on the statical model [23–27].

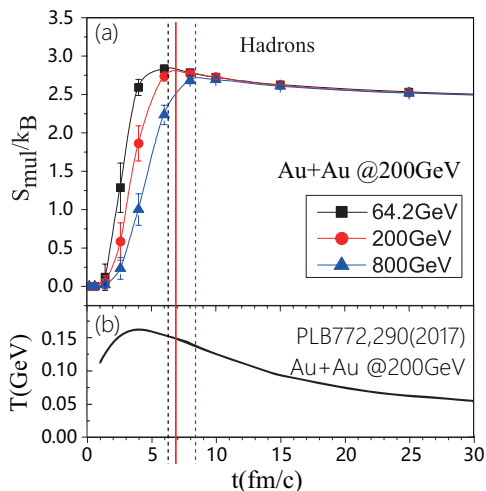


FIG. 5: (a) Time evolution of the Multiplicity entropy in the hadronic phase of central Au+Au collisions at $\sqrt{s_{NN}} = 200$ GeV, as well as, (b) the extracted temperature from the hadron resonance gas model.

It should be noted that the critical point obtained by the multiplicity entropy is very close to the starting

point of the linear increase of the thermodynamic entropy, which indicates that the chaotic degree of the system increases sharply after the system evaporates from QGP state to hadronic gas. The critical point will be reached later at higher c.m. energies, due to the higher temperature in the central region at higher c.m. energies. Thus the cooling time of QGP into hadronic gas will be longer. After the critical point, the multiplicity entropy of hadrons decreases gradually to a stable value, which reflects the decay of unstable excited hadrons into more stable hadrons.

The multiplicity entropy of the whole system is also plotted in Fig. 4(c), but this result is unsatisfactory for the prediction of critical point. The reason for this defect is that the particles in the global region can not correspond to those particles in the region where the phase transition actually occurs, while the region where the hadron is produced corresponds to the region where the phase transition occurs. Therefore, it is more accurate to determine the critical point by using the hadron multiplicity entropy.

V. THE CONFIGURATION ENTROPY

In the previous studies, we regard both partons and hadrons as point particles without internal structure, but in fact mesons and baryons are composed of quarks, in which the mesons are composed of two quarks and most baryons are composed of three quarks. For mesons consisting of two quarks, there is only one space configuration, but for baryons consisting of three quarks, the internal space configuration is not clear. It should be noted here that after nuclear collision, the system will inevitably be accompanied by changes in the amount of information in the process from point particles without internal structure to nucleons with internal structure. Here we attempt to quantify the information variable caused by the change of particle internal configuration.

Inspired by the work of Csernai et al. [16], we consider that particles consisting of three nucleons have four possible configurations, each of which has a different probability of formation, which is related to: direction dependence of the links, different constituents, different (energetic) weights of the links, dynamical freedom of the length or angle of the link, etc. In this way, we can get the corresponding topological Shannon entropy through the probability distribution of different binding modes of quarks in nucleon.

It is interesting that the quark-diquark model mentioned by Lichtenberg [17, 28, 29] in 1982 coincides with the above viewpoint. This model described baryon as a bound state of one quark with one diquark, in which the diquark is formed by the attraction of two quarks with color and spin anti-symmetry, when both quarks are correlated in this way they tend to form a very low energy configuration. In this model, there are four possible configurations inside baryons (we only consider those particles with quark numbers less than or equal to 3).

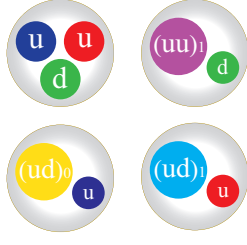


FIG. 6: The 4 internal configurations of proton based on the Di-quark model.

For example, the four internal configurations of protons are shown in Fig. 6. Here we assume equal probability for each topological configuration in baryon, so that the probability of any configuration in baryons is $1/4$. However, we also need to consider that there are other particles with only one internal configuration in the collision process, so there are:

$$p_{\text{baryon}} = \frac{N_{\text{baryon}}}{N}, \quad p_{\text{others}} = 1 - p_{\text{baryon}}. \quad (2)$$

Then the configuration entropy of system is:

$$S_{\text{conf}} = (p_{\text{others}}) \ln(p_{\text{others}}) + 4 * \left[\frac{p_{\text{baryon}}}{4} \ln\left(\frac{p_{\text{baryon}}}{4}\right) \right]. \quad (3)$$

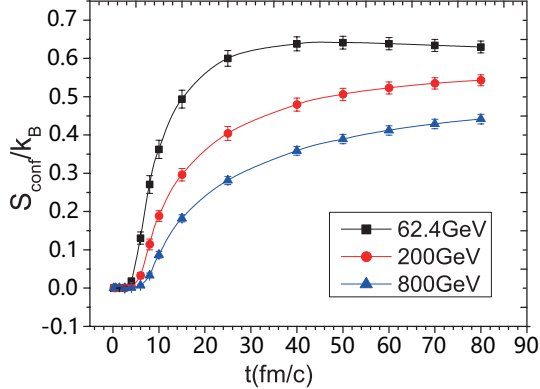


FIG. 7: Time evolution of configuration entropy of system in Au+Au collisions at different energies.

The configuration entropy of system in Au+Au collisions at different c.m. energies is plotted in Fig. 7. One can see that the time evolution of configuration entropy at different c.m. energies are similar in Fig. 7. The configuration entropy of a collision system with a higher c.m. energy is lower than that of a collision system with a lower c.m. energy, because higher c.m. energies collide to produce a larger proportion of mesons without internal structures.

Above all, we have calculated the thermodynamic entropy, multiplicity entropy, and configuration entropy of a Au+Au collision system at different c.m. energies of 64.2 GeV, 200 GeV, and 800 GeV, respectively. Now we

need to rethink that what characteristics of a Au+Au collisions at the RHIC energy are showing by these different kinds of entropy.

In C.W. Ma's review [4], "the basic scientific meaning of Shannon information entropy applied in heavy-ion collisions is to indicate the chaoticity of nuclear matter in the colliding nuclear system" is mentioned. This reminds us that all three kinds of entropy, including from dynamic phase space, particle type and internal configuration of particles, reflect the chaotic nature of the system in the evolution of relativistic heavy ion collisions. This enlightens us that a complete description of the degree of chaos in the evolution of relativistic heavy ion collision system should include as much information entropy changes as possible in different aspects. The cumulative values of the above three kinds of entropy are calculated under this idea. The results of the total entropy S ($= S_{\text{thermal}} + S_{\text{mul}} + S_{\text{conf}}$) of the system during the evolution of Au+Au collisions are shown in Fig. 8, where the time development appear smooth.

From Fig. 8, we can see that the time evolution of the total entropy in the Au+Au collisions system goes through four stages: The first stage, about $0 < t < 3$ fm, entropy decreases due to the energy released by string formation and melting and compression after collision; Second, entropy is at the minimum of the system about $3 < t < 5$ fm, corresponding to the parton rescattering phase, which the system is in the quark gluon plasma (QGP) state; Then the entropy of the system increases rapidly from $t = 5$ fm to 9 fm, which may correspond to the transformation process from QGP to hadron phase; After that, the entropy distribution tends to be saturated, which would correspond to state of hadron scattering. In addition, the higher the c.m. energy in the Au+Au collision, the faster the entropy of the system reaches the equilibrium state. This is because the particles produced by collisions with higher energies have higher momentum, which makes the system approach the maximum disorder faster.

Following the reference [16], it is important to mention that, (1) all degrees of freedom should be taken into account, (2) these should be independent degrees of freedom (orthogonal), (3) the degrees of freedom must be quantized, also for continuous degrees of freedom. This last point was recognized after the development of quantum mechanics, which led to the quantization of phase-space volume cells. Point (1) is violated in this AMPT evaluation on the string degrees of freedom are not taken into account and this led to a temporary decrease of the total entropy. Such decrease should not happen in a closed system. This missing entropy of string is shown clearly in Fig. 8

In this letter, the time evolution process of thermodynamic entropy S_{thermal} , multiple entropy S_{mul} , and configuration entropy S_{conf} in relativistic heavy ion collision is studied carefully using AMPT model to generate central Au+Au collisions at $\sqrt{s_{NN}} = 200$ GeV with $|y| < 1$

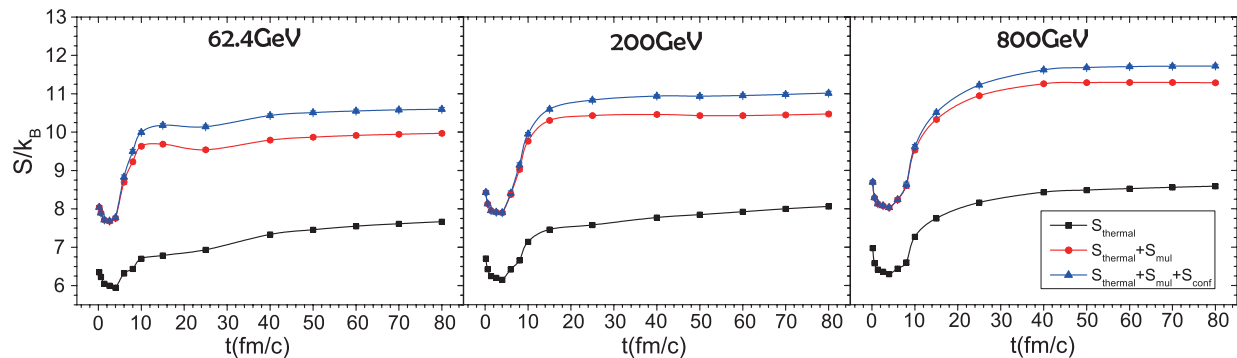


FIG. 8: Time evolution of total information entropy for system in Au-Au collisions at different c.m. energies.

and $p_T < 5$ acceptances. In this way, we obtain the time evolution distribution image of the total entropy S in the relativistic heavy ion collision. The results show that the four stages of the time evolution process of the system entropy S have obvious correspondence with the four physical processes experienced in the relativistic heavy ion collision, indicating that the total entropy of the system can more accurately reflect the physical information in the relativistic heavy ion collision.

Acknowledgments

The authors thank Prof. Laszlo P. Csernai and Prof. Che Ming Ko for valuable comments, thank Ph.D. L.

Zheng, Z.L. She, and Z.J. Dong for useful discussion about AMPT. This work is supported by the National Natural Science Foundation of China(11475149).

VI. REFERENCES

- [1] L. Turko, *Universe* **4**, 52 (2018).
- [2] K. Werner, *High Energy Physics. Phenomenology* (2001).
- [3] L. Csernai and J. I. Kapusta, *Physics Reports* **131**, 223 (1986).
- [4] C.-W. Ma and Y.-G. Ma, *Progress in Particle and Nuclear Physics* **99**, 120 (2018).
- [5] L. Boltzmann, *Lectures on gas theory* (Courier Corporation, 2012).
- [6] L. Boltzmann, in *History of Modern Physical Sciences* (2003), pp. 262–349, originally published under the title “Weitere Studien ber das Wärmegleichgewicht unter Gasmoleklen”, in *Sitzungsberichte Akad. Wiss., Vienna*, part II, 66, 275370 (1872); reprinted in Boltzmann’s *Wissenschaftliche Abhandlungen*, Vol. I, Leipzig, J. A. Barth, 1909, pp. 316402, URL https://www.worldscientific.com/doi/10.1142/9781848161337_0015.
- [7] E. T. Jaynes, *American Journal of Physics* **33**, 391 (1965).
- [8] W. H. Cropper, *Great physicists: The life and times of leading physicists from Galileo to Hawking* (Oxford University Press, 2001), for those interested in the history of entropy in thermodynamic and statistical mechanics, it’s a good choice to read the chapters of thermodynamic and statistical mechanics in this book, pp.93-123&177-200.
- [9] C. E. Shannon, *Bell System Technical Journal* **27**, 379 (1948).
- [10] M. S. Longair, *Theoretical concepts in physics* (University Press, 1984), ISBN 0521821266, chapter 10 :Kinetic theory and the origin of statistical mechanics.
- [11] Z. Cao and R. C. Hwa, *Physical Review D* **53**, 6608 (1996).
- [12] Y.-G. Ma, *Physical Review Letters* **83**, 3617 (1999).
- [13] C.-W. Ma, H.-L. Wei, S.-S. Wang, Y.-G. Ma, R. Wada, and Y.-L. Zhang, *Physics Letters B* **742**, 19 (2015).
- [14] C.-W. Ma, Y.-D. Song, C.-Y. Qiao, S.-S. Wang, H.-L. Wei, Y.-G. Ma, and X.-G. Cao, *Journal of Physics G: Nuclear and Particle Physics* **43**, 045102 (2016).
- [15] J. Xu and C. M. Ko, *Physics Letters B* **772**, 290 (2017).
- [16] L. Csernai, S. Spinnangr, and S. Velle, *Physica A: Statistical Mechanics and its Applications* **473**, 363 (2017).
- [17] D. B. Lichtenberg, W. Namgung, E. Predazzi, and J. G. W. Wilson, *Physical Review Letters* **48**, 1653 (1982).
- [18] Z.-W. Lin, C. M. Ko, B.-A. Li, B. Zhang, and S. Pal, *Physical Review C* **72** (2005), the latest source code for AMPT is on the website: <http://myweb.ecu.edu/linz/amp/>.
- [19] X.-N. Wang and M. Gyulassy, *Physical Review D* **44**, 3501 (1991).
- [20] B. Zhang, *Computer Physics Communications* **109**, 193 (1998), URL <https://www.sciencedirect.com/science/article/pii/S0010465598000465>.
- [21] B.-A. Li and C. M. Ko, *Physical Review C* **52**, 2037 (1995).

- (1995).
- [22] Y. Meiling, D. Jiaxin, and L. Lianshou, *Physical Review C* **74**, 6 (2006).
 - [23] J. Adams, M. Aggarwal, Z. Ahammed, J. Amonett, B. Anderson, D. Arkhipkin, G. Averichev, S. Badyal, Y. Bai, J. Balewski, et al., *Nuclear Physics A* **757**, 102 (2005).
 - [24] K. Adcox, S. Adler, S. Afanasiev, C. Aidala, N. Ajitanand, Y. Akiba, A. Al-Jamel, J. Alexander, R. Amirikas, K. Aoki, et al., *Nuclear Physics A* **757**, 184 (2005).
 - [25] L. Adamczyk, J. K. Adkins, G. Agakishiev, M. M. Aggarwal, Z. Ahammed, N. N. Ajitanand, I. Alekseev, D. M. Anderson, R. Aoyama, A. Aparin, et al., *Physical Review C* **96** (2017).
 - [26] J. Cleymans, H. Oeschler, K. Redlich, and S. Wheaton, *Physical Review C* **73** (2006).
 - [27] A. Andronic, P. Braun-Munzinger, and J. Stachel, *Nuclear Physics A* **834**, 237c (2010).
 - [28] R. Rapp, T. Schäfer, E. Shuryak, and M. Velkovsky, *Physical Review Letters* **81**, 53 (1998).
 - [29] M. Tanabashi, K. Hagiwara, K. Hikasa, K. Nakamura, Y. Sumino, F. Takahashi, J. Tanaka, K. Agashe, G. Aielli, C. Amsler, et al. (Particle Data Group), *Phys. Rev. D* **98**, 030001 (2018), chapter34:Monte Carlo particle numbering scheme, URL <https://link.aps.org/doi/10.1103/PhysRevD.98.030001>.